# Asymmetric Nafion/(Zirconium Oxide) Hybrid Membranes via *In Situ* Sol-Gel Chemistry

W. APICHATACHUTAPAN, R. B. MOORE, and K. A. MAURITZ*

Department of Polymer Science, University of Southern Mississippi, Hattiesburg, Mississippi 39406-0076

**SYNOPSIS**

Nafion-*in situ* sol-gel reactions were affected for $Zr(OBu)_4$ that permeated low water content membranes unidirectionally. IR peaks reflecting $ZrO_2$ and incomplete hydrolysis of ZrOBu groups near both surfaces were detected. Vibrations of $Zr(OEt)_4$ detected near both sides arise from alkoxy exchange in the presence of the solvent EtOH. Unreacted alkoxy group bands are more distinct near the nonpermeated surface. An IR band for the ZnOBu group diminishes, whereas that for ZnOEt increases with increasing time near the permeated surface due to progressive alkoxy exchange. The $ZrO_2$ band becomes more intense with time near the permeated surface. X-ray spectroscopy/scanning electron microscopy studies of Zr concentration across the membrane thickness verified compositional asymmetry. $CO_2$ gas permeability versus upstream pressure plots are monotonically increasing, suggesting diffusion accompanied by complex plasticization. © 1996 John Wiley & Sons, Inc.

## INTRODUCTION

The synthesis of zirconium alkoxides and the formation of $ZrO_2$ from these compounds was reported by Bradley and colleagues[1-3] and Mazdiyazni et al.,[4,5] respectively. Compared with silicon alkoxides, hydrolysis and condensation reactions of Zr alkoxides occur rapidly because Zr has a lower electronegativity and an ability to form several coordination states upon reaction with water.[6] Bradley and Carter[7,8] noted that hydrolysis of primary zirconium alkoxides leads to polymeric oxide-alkoxides, i.e., $[ZrO_x(OR)_{4-2x}]_n$. Although the multiple reactions are complex, the following minimal overall two-step scheme was discussed by Mazdiyazni et al.[4]:

$$Zr(OR)_4 + H_2O \rightarrow ZrO(OR)_2 + 2R(OH)$$

$$2ZrO(OR)_2 \rightarrow ZrO_2 + Zr(OR)_4 \qquad (1)$$

As this reaction does not lead to hydroxides, as also discussed by Yoldas,[9,10] the hydrolysis-condensation of Zr alkoxides differs fundamentally from that of Si, Al, and Ti. Pierre and Uhlmann[11] state that once one OR group in $Zr(OBu)_4$ is replaced by one OH group according to the classic hydrolysis reaction, this OH group will tend to react with a second OR group, leading to a $ZrO_2 \cdot nH_2O$ gel based on $ZrO(OR)_2$ units.[12] The hydrolysis reaction in this system leads to the formation of oxo-groups ($Zr{=}O$) and aquo-groups ($Zr{-}(OH_2)$) rather than to true hydroxides. Diffusion and statistical interactions control molecular weight distribution and resultant particle morphology.[10] As opposed to gels produced by the hydrolysis → condensation of tetraethoxysilane, the reactions of $Zr(OR)_4$ can lead to crystalline materials.

However, Harris et al.[13] mention that reaction scheme (1) is based on experiments in which the water-to-alkoxide ratio was less than 2. For higher ratios, the following scheme, presented by Kundu and Ganguli,[14] similar to the usual representation of sol-gel reactions, may be more appropriate:

$$Zr(OR)_4 + mH_2O \rightarrow Zr(OR)_x(OH)_y + yROH$$

$$Zr(OR)_x(OH)_y \rightarrow$$

$$ZrO_z(OR)_{x1}(OH)_{y1} + (x - x_1)ROH \qquad (2)$$

* To whom correspondence should be addressed.

Journal of Applied Polymer Science, Vol. 62, 417-426 (1996)
 CCC 0021-8995/96/020417-10

where $z = [4 - (x_1 + y_1)]/2$. In this scheme, hydroxides are present. In any case, although interesting structures have been created via the sol-gel reaction for Zr alkoxides, it might be said that reaction mechanisms remain ubiquitous to a degree.

In the work reported here, sol-gel reactions of $Zr(OBu)_4$ were conducted within the nanophase-separated environment[15] of Nafion ionomer membranes. This work is a continuation of our efforts to create Nafion/[inorganic oxide] nanocomposite membranes wherein the composition profile of the inorganic phase across the film thickness is asymmetric. Earlier, Gummaraju[16] produced asymmetric Nafion/[silicon oxide] films. In this prior effort, the molecular connectedness of the silicon oxide phase was characterized using IR spectroscopy. X-ray spectroscopy/scanning electron microscopy (EDAX/SEM) verified silicon oxide compositional asymmetry across the film thickness, and gas permeation experiments indicated a dual mode sorption that reflected the multiphase morphology of these hybrid materials.

The work reported here deals with affecting Nafion-*in situ* sol-gel reactions for tetrabutylzirconate (TBZ) that permeated these membranes from alcohol solutions contacting only one side for prescribed times at room temperature. As in our earlier efforts dealing with Nafion/$SiO_2$ hybrids,[17–19] and later Nafion/($SiO_2$-$TiO_2$), Nafion/($SiO_2$-$Al_2O_3$),[20,21] and Nafion/ORMOSIL hybrids,[22–24] our working hypothesis was the following: the quasi-ordered nanophase-separated morphology of this ionomer acts as a polymerization template that directs the ultimate morphology of dried *in situ* gel nanostructures. FT-IR, EDAX/SEM, and gas permeability techniques were used to analyze the resultant Nafion/$ZrO_2$ hybrids.

We envision that composition gradients within these nanocomposites will generate gradients of material properties, e.g., index of refraction, dielectric constant, $T_g$, and mechanical properties. Inorganic oxide phases might serve as platforms for molecules having nonlinear optical properties. The scale of structural heterogeneity is much smaller than the wavelength of light so that scattering losses would be minimal. Asymmetric Nafion/[inorganic oxide] membranes might discriminate between diffusants on the basis of molecular size exclusion from inorganic oxide nanopores, as well as on the basis of energetic preference. Inorganic oxide nanophases might also serve as supports on which catalytic metal clusters can be deposited.

## EXPERIMENTAL

### Nafion/[Zirconium Oxide] Hybrid Formulation

All 5-mil thick, 1100 equivalent weight, $SO_3H$-form Nafion membranes, supplied by E. I. DuPont Co., were initialized and vacuum dried at 100°C for 36 h. The detailed initialization procedure, described by Davis et al.[25] in an earlier report, consists of steps involving exchanging the membranes to the acid form in aqueous HCl and $HNO_3$ solutions, leaching out excess acid in deionized water, and vacuum drying the water-swollen membrane. The initialized membranes were stored in deionized $H_2O$ until they were modified by the *in situ* sol-gel reaction, as follows. First, the membranes were boiled in water for 30–60 min followed by drying at 50°C for 4 h. The mild drying step served to remove some, but not all, loosely bound water. Owing to the fast reaction of TBZ, it was desired to limit, in part, the amount of hydrolysis water in the membrane in this way. Then, these samples were immersed in solutions of $H_2O$/EtOH = 1/10 (v/v) (~ 5.65 wt % $H_2O$) for 1 h and then removed. EtOH serves to swell Nafion to facilitate sorption of TBZ. Incorporated $H_2O$ hydrolyzes incoming TBZ and initiates the *in situ* sol-gel reaction that is assumed to occur within the nanometers-in-size sulfonic acid clusters wherein the acid sites catalyze alkoxide hydrolysis.

A given alcohol-water swollen film was immediately mounted in a liquid cell designed for one-sided permeation. One side of the membrane was exposed to a TBZ solution and the other to air. Zr(IV)*n*-butoxide and EtOH were premixed in a separate container for the dilute concentration TBZ : EtOH = 1 : 40 (v/v). A given stirred TBZ solution was introduced to the cell chamber and the permeation + *in situ* sol-gel reaction was allowed to proceed for 5 min at room temperature, after which time the solution was drained. Having removed the membranes from the cell, their surfaces were rinsed with fresh EtOH to remove adherent TBZ and its hydrolyzed and oligomerized species to prevent the undesired precipitation of $ZrO_2$. Samples were dried in air for 3 h and finally vacuum-dried at 100°C for 24 h to remove volatiles and promote further condensation reactions. In subsequent experiments, permeation-reaction time was increased to 10, 15, and 20 min, all for the concentration TBZ : EtOH = 1 : 40 (v/v), or 1 : 311 mol/mol, with the other steps being the same as before.

TBZ was used in dilute quantity to slow the sol-gel reaction in the near-surface regions. Optical mi-

croscopic inspection of the surfaces of treated membranes in fact did not reveal zirconia precipitates. Although the exact quantity of water in the membrane is unknown, the above procedure clearly reduces the amount considerably from that used in our previous Nafion *in situ* sol-gel reaction schemes. Figure 1 roughly depicts the Nafion/$ZrO_2$ hybrid formulation sequence.

On visual inspection, all samples are of good quality, transparent, and free of surface-attached $ZrO_2$ layers as verified by optical microscopy. Excluding the first entry, the uptake increases with increasing permeation-reaction time. The sample prepared for gas permeation evaluation had a permeation-reaction time of 10 min.

## IR Spectroscopy

Owing to the high IR absorbance of these membranes, transmission studies are not possible, and FT-IR spectra were collected in attenuated total reflectance (ATR) mode. A Bruker IFS 88 FT-IR spectrometer was utilized and 500 scans used to obtain each spectrum. Operating in ATR mode allows for probing molecular composition and structure in the near-surface regions. Owing to the asymmetric distribution of the zirconium oxide phases, ATR is in fact the mode of choice.

Subtraction spectra were obtained, i.e., (dried Nafion-$H^+$/[zirconium oxide] spectrum) − (dried Nafion-$H^+$ spectrum). Both membranes were taken from the same lot in each case. This subtraction was performed to observe peaks characteristic of the zirconium oxide phase to the exclusion of the numerous interfering bands characteristic of pure Nafion.[26]

## Energy Dispersive Analysis by EDAX

The EDAX attachment of an Electroscan environmental scanning electron microscope (ESEM) was used to determine Zr composition profiles across the thickness direction of these films. If an electron beam is focused on a small sample area, e.g., 1 $\mu m^2$, analysis of emitted X-rays permits determination of relative elemental composition in that area.

Hybrid films were freeze-fractured in liquid $N_2$ so that a fresh cross-sectional surface could be probed point-by-point along the thickness direction (thickness ~ 0.13 mm). The intensity of the sulfur line was used as an internal concentration standard, being a measure of $SO_3^-$ density. Zr/S intensity ratio was then considered to represent relative quantity

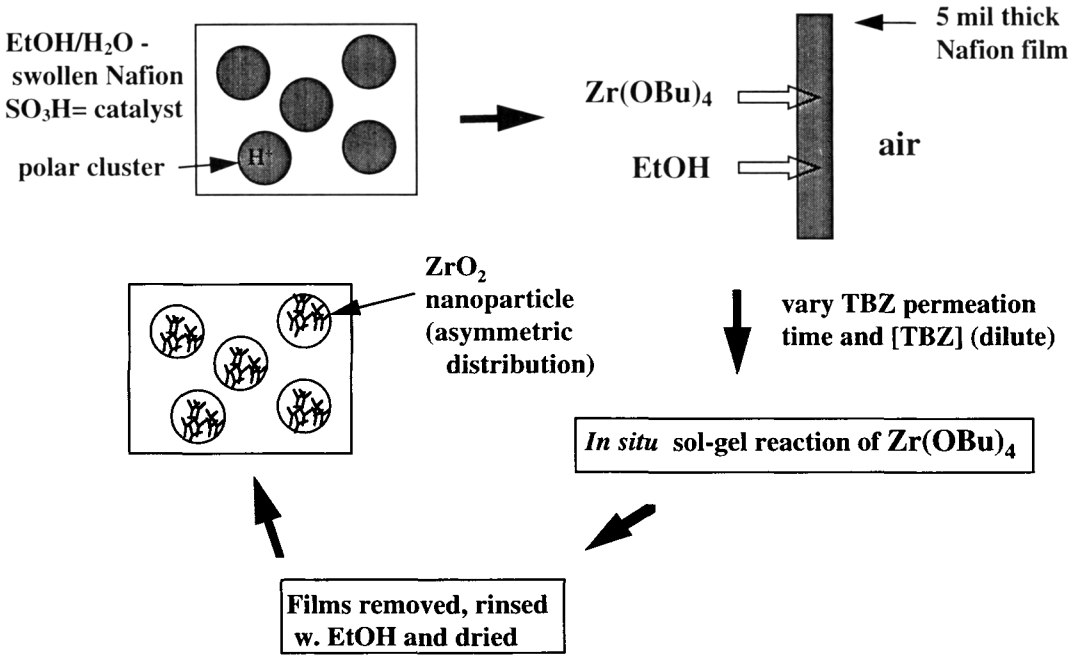


**Figure 1** Schematic depiction of Nafion/[zirconium oxide] nanocomposite formulation via *in situ* sol-gel reactions that initiate within nanometers-in-size EtOH + $H_2O$-containing sulfonic acid clusters.

of zirconium oxide in the selected region. The data obtained was subjected to the ZAF correction procedure and can be used for semiquantitative analysis.

### Gas Permeation Studies

In these initial studies, the $CO_2$ permeability coefficient ($P$) of these hybrid membranes was determined using the steady-state method. Future studies will involve other gas molecules of varying sizes and polarities. $CO_2$ was chosen because it was thought to interact strongly with polar groups on incorporated zirconium oxide nanostructures. Owing to the low zirconium oxide uptakes seen in Table I, it was thought that diffusion of a polar gas would be influenced more strongly than that of a nonpolar gas by the inorganic phase. These preliminary permeation investigations are meant to indirectly probe free volume and nanophase separation. In future studies, test gases will be selected on the basis of probing specific energetic environments.

Room temperature experiments were performed using a Custom Scientific CS-135 constant pressure permeability cell console that we modified to accommodate smaller samples. The gasketed two-compartment cells were placed in an isothermal water bath to avoid temperature drift due to air fluctuation. The permeated-reacted side of the membrane was subjected to a gas pressure $p$ and the downstream nonpermeated side exists at atmospheric pressure. For a given $p$, the cumulative volume of gas ($V$) transported to the downstream side and into a chamber is monitored as a function of time ($t$). In the initial stages, as concentration of gas in the membrane is accumulating, $V$ versus $t$ plots are concave upward, but eventually the plot is linear when the steady state is achieved, i.e., equal volumes of gas are transported in equal time intervals. $V$ is determined by monitoring the displacement, by downstream gas, of a slug of dye in an open vertical glass capillary of known inner diameter.

The sequence of steps in the gas permeation experiment was as follows. After collecting $V$ versus $t$ data at a fixed temperature and given $p$, $p$ was incremented upward by a specified amount and $V$ versus $t$ data collected again, etc. Steady-state slopes for slug height versus $t$ graphs and the capillary bore cross-sectional area were used to calculate $q$, the volume flowrate, i.e., gas volume (STP)/time. $P$ is then calculated from the following equation based on Fick's First Law:

$$P = qd/(A\Delta p) \tag{3}$$

**Table I Percent Zirconium Oxide Uptake, Overall Internal Zr/S EDAX Intensity Ratio Versus Permeation-Reaction Time for TBZ : EtOH = 1 : 40**

| TBZ Permeation Time (min) | $ZrO_2$ Uptake (wt %) | Zr/S |
|---|---|---|
| 5 | 2.13 | 0.090 |
| 10 | 0.29 | 0.015 |
| 15 | 0.39 | 0.048 |
| 20 | 1.15 | 0.079 |

In eq. (3), $A$ is the effective area of the membrane surface across which the gas flows (1.0 in. C.D.), $d$ is the membrane thickness measured with a micrometer, and $\Delta p$ the constant pressure drop across the thickness. As gauge pressures are used, $\Delta p$ is essentially equal to $p$. Using CGS units, $P$ is expressed in units of Barrers.

$P$ calculated according to eq. (3) should be viewed as an average over the ensemble of microstructural heterogeneity in the sense that a local value of $P$ on the TBT-permeated side will be different than the value on the opposite side.

First, the membranes, which were stored in a dessicator before use, were purged by $CO_2$ without the dye slug in the capillary tube for 3 h. Afterward, the slug was injected into the tube and $CO_2$ gas passed again through the membrane for 15–40 min during the time-lag period preceding steady state. Four different upstream pressures were used: 40, 60, 75, and 100 psig (2.72–6.80 atm).

## RESULTS AND DISCUSSION

### IR Spectroscopy

The following vibrations are reported as characteristic of zirconium oxide structures. According to Nogami,[27] a band in the region 500–600 $cm^{-1}$ exists for $ZrO_8$ groups in which $Zr^{4+}$ ions are not present in the total anionic framework structure of the glass. Lee and Condrate[28] discuss an IR band $\sim$ 600 $cm^{-1}$ indicative of cubic zirconia-type $ZrO_8$ units in a zirconia-rich glassy phase. A rather broad band at 490 $cm^{-1}$ was reported by McDevitt and Baun[29] for cubic-stabilized zirconia and, based on this evidence, Sim et al.[30] suggested that a band detected $\sim$520 $cm^{-1}$ for $ZrO_2$-SiC whisker composite coatings was also due to this mode. Although the exact wave

number and intensity of a vibrational mode involving Zr — O bonds depends on details of the arrangements of oxygen atoms around Zr atoms (e.g., $ZrO_4$, $ZrO_6$, monoclinic zirconia-type $ZrO_7$, tetragonal zirconia-type $ZrO_8$, cubic zirconia-type $ZrO_8$ units), this band around 600 $cm^{-1}$, in a general sense, signals the presence of zirconia. For the $Zr(OBu)_4$ monomer, the $\upsilon$(C — O)Zr and $\upsilon$(Zr — O) stretching modes occur around 997 and 540 $cm^{-1}$, respectively.[1]

Difference spectra are displayed in Figure 2 for the permeated-reacted side of the hybrid membranes. There is in fact a major broad envelope around 600 $cm^{-1}$ that reflects the presence of a zirconium oxide compound. The considerable width of this envelope might be attributed in a general way to a broad distribution of zirconium oxide molecular structure. This band understandably becomes more intense with increasing time while the absorbance distribution shifts to lower wave numbers. $\upsilon$(C — O)Zr for TBZ is clearly present in all spectra, indicating incomplete monomer hydrolysis and/or ZrOBu groups on larger condensed structures. The above-cited $\upsilon$(Zr — O) band for unreacted TBZ at 540 $cm^{-1}$ is also present as a low frequency shoulder on the stronger $ZrO_2$ band. We also note that Bradley et al.[1] list strong bands for TBZ, of unspecified vibrational modes, in the region 1160–1134 $cm^{-1}$; such absorbances are evident in Figure 2, as well.

There are peaks characteristic of $Zr(OEt)_4$ in the spectra. C — O vibrations of medium intensity for tetraethylzirconate (TEZ) are known to exist in the range 1095–918 $cm^{-1}$.[1] Two and possibly three bands are in this region in Figure 2. The smaller overall mass attached to the O atom in this bond for TEZ, relative to TBZ, accounts for the shift to higher wave numbers for ethoxy substitution. As the carrier solvent is ethanol, the most obvious suggestion is that the appearance of TEZ bands is due to the exchange reaction:

$$Zr(OBu) + EtOH \rightarrow Zr(OEt) + BuOH \quad (4)$$

Of course, this exchange would also increase the rate of hydrolysis owing to diminished steric effects. The C — O stretching band for the ZnOBu group diminishes and that for the ZnOEt group is correspondingly enhanced, with increasing permeation-reaction

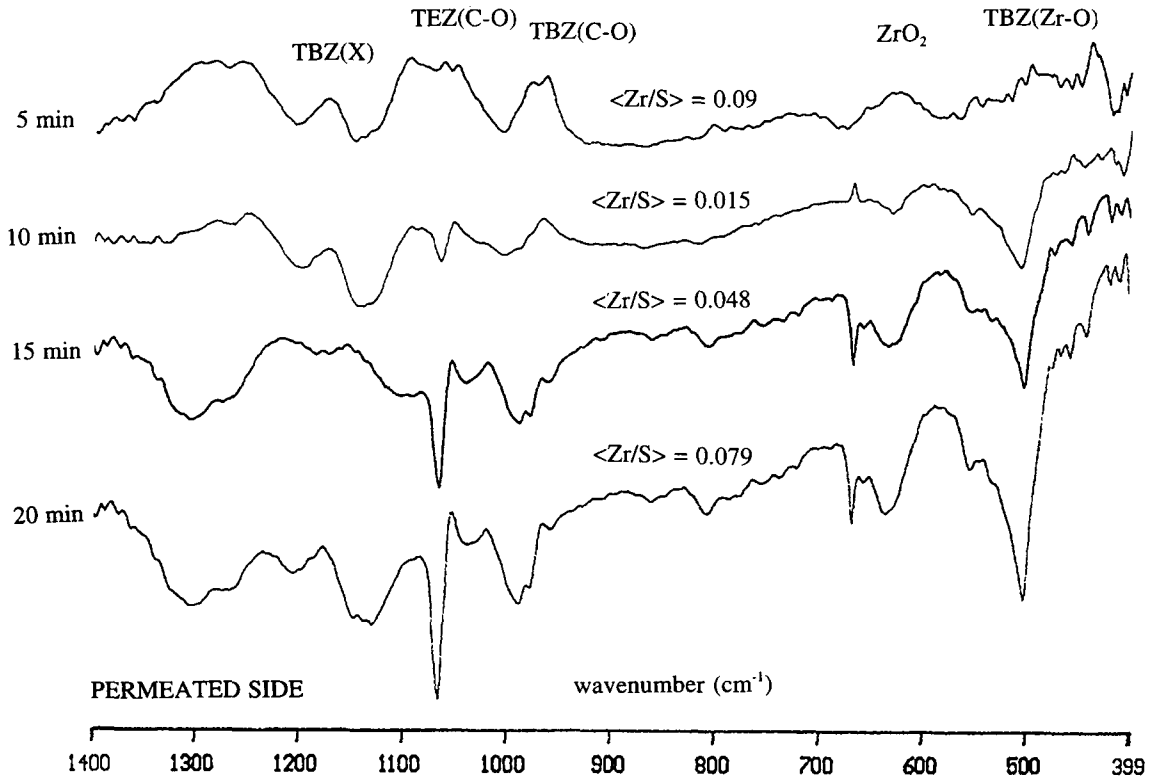


**Figure 2** FT-IR/ATR difference spectrum of TBZ-permeated side of Nafion/[zirconium oxide] membranes versus TBZ permeation time.

time, which is reasoned in terms of the progress of reaction (4).

Figure 3 shows spectra for the corresponding unpermeated sides. Comments essentially identical to those relating to the permeated side can be made for these spectra. It is noted, however, that the bands reflecting unreacted alkoxy groups of both kinds appear to be more distinct toward the nonpermeated side. We offer the following explanation for this phenomenon. At the onset of unidirectional TBZ permeation, the initial water concentration profile is symmetric because in the previous step $H_2O$/MeOH was sorbed into both sides of the membrane in equal fashion. However, water is consumed in the initial stages by hydrolysis reactions toward the permeated side. Owing to the fact that, in the initial stages, water is undisturbed near the nonpermeated side, an $H_2O$ concentration or activity gradient is generated that drives water toward the permeated side with the result that there are fewer $H_2O$ molecules available for hydrolysis toward the nonpermeated surface.

It is remarkable, considering that this is the unpermeated side and the overall uptakes are rather low, that the bands are well-defined. No zirconia precipitate was noted on the surface that would exaggerate the zirconium oxide bands.

Thus, zirconium oxide compounds, in presently unknown polymerized or oligomerized bonding states, are present in both near-surface regions, although unhydrolyzed butoxy and ethoxy groups persist in both regions. These two results are due to the fact that hydrolysis water is present in low, albeit unknown quantity, compared with the amount present in our earlier formulations of similar hybrids. The condition of dilute TBZ concentration in the external feed solution might limit the size of synthesized zirconium oxide structures that are hypothesized to grow in the sulfonic acid cluster domains. The fact that alkoxides traverse the entire film thickness, evidenced by their IR detection in the near surface regions of the unpermeated side, implies fast diffusion compared with the rate of reaction for these species. This evidence must be evaluated alongside the Zr elemental profiles along the thickness direction established by EDAX/ESEM, which is discussed later.

## EDAX Analysis

Figure 4 illustrates a typical Zr/S distribution across the film thickness for 5 min permeation-reaction time. $\langle Zr/S \rangle$, the "average" ratio noted in Figure 4, is obtained by selecting an area for X-ray microanalysis that spans the distance between the surfaces but does not include the surfaces. The main conclusion is that zirconium oxide composition profiles are indeed asymmetric, greatly biased toward the permeated surface, and that Zr is essentially undetected near the nonpermeated side in most cases. Other experiments indicate that Zr accumulation in the near-surface regions increases with increasing TBZ feed solution concentration, as is reasonable. The primary goal of these preliminary investigations was to ascertain whether an asymmetric zirconium oxide phase can be affected under these experimental conditions; this goal has been achieved. It is interesting that although EDAX does not detect Zr near the nonpermeated surfaces, FT-IR/ATR spectroscopy does.

We offer the following mechanistic interpretation of the profile in Figure 4. TBZ is sorbed, diffuses inward, and after these molecules encounter and react with $H_2O$ water molecules, oligomers grow by condensation reactions. When these larger oligomers reach a certain size, they become immobile. Subsequent-diffusing TBZ molecules will react with these in-place structures that pose obstacles for diffusion that accounts for the effective reduction of Zr/S even before the middle of the film is reached.

## Gas Permeation

Figure 5 is a typical example of dye slug height in the vertical capillary tube versus time of $CO_2$ permeation. In this case, $p$ = 60 psig (4.08 atm) and the temperature is 24.5°C. As discussed, $q$ = volume flowrate is derived from the slopes of these lines knowing the tube diameter. This and all other plots are extremely linear and reproducible. The fact that linearity is observed over times that are considerably longer than those plotted in Figure 5 indicates the existence of a physically and chemically stable steady-state diffusion regime.

In Figure 6 is the $P$ versus $p$ plot where each point is derived from an entire graph such as that in Figure 5. $P$ monotonically increases with increasing $p$; this result is reproducible. This upward trend is opposite to that observed in our similar studies of Nafion/[silicon oxide] asymmetric membranes in which the permeant was He rather than $CO_2$.[16] In this earlier study, $P$ versus $p$ curves showed an inverse relationship that was attributed to a dual mode sorption diagnostic of the multiphasic nature of these hybrids.

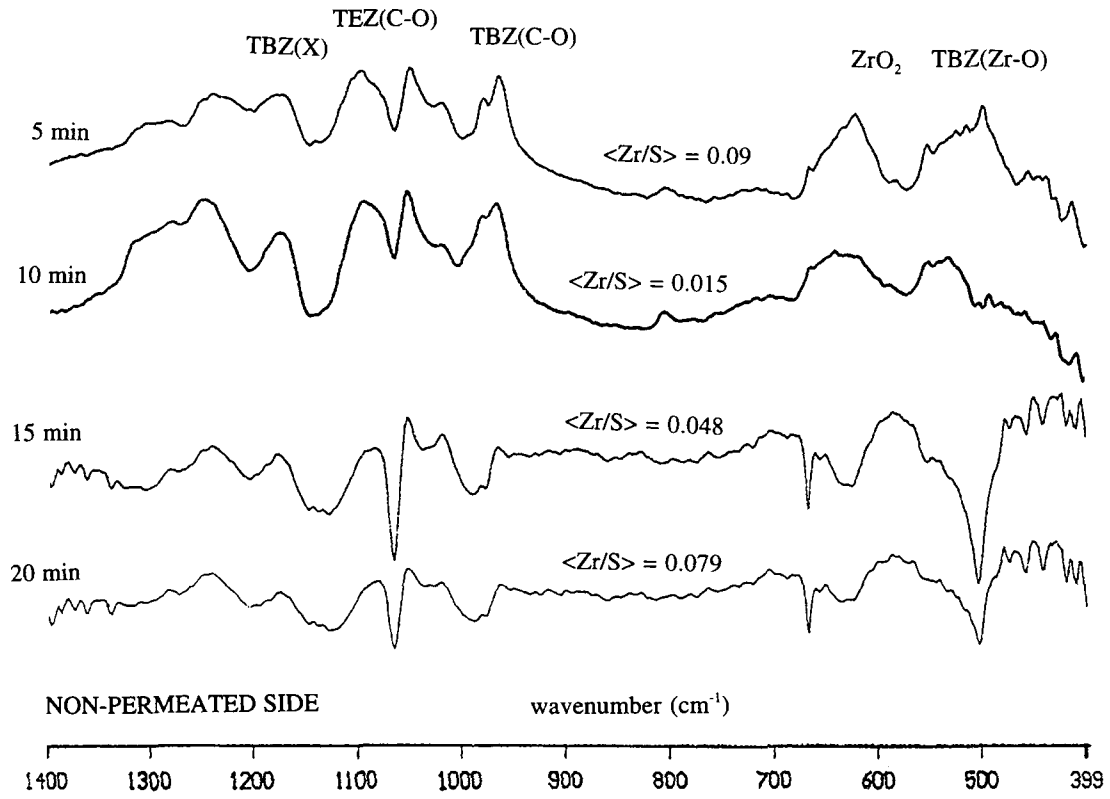


**Figure 3** FT-IR/ATR difference spectrum of nonpermeated side of Nafion/[zirconium oxide] membranes versus TBZ permeation time.

The behavior in Figure 6 is akin to that of diffusion within plasticized polymers wherein sorbed molecules strongly interact with polymer chains to create additional free volume, thereby increasing chain segmental mobility. As in our earlier studies,[16] the gas sorption isotherm might be represented as the sum of a Henry's Law term involving dissolution in the polymer matrix and a Langmuir adsorption-like term. Within the context of these multiphasic materials, the Langmuir term accounts for the filling of voids in the nanometers-in-size clusters by gas molecules. For the Nafion/[zirconium oxide], as opposed to the Nafion/[silicon oxide] hybrid, the dissolution term predominates. We offer the following mechanism, speculatively, that is more complex than that of direct plasticization of the amorphous perfluorocarbon regions by interactive $CO_2$ molecules.

Under increasing pressure, more $CO_2$ molecules flood the clusters and collide with the domain boundaries owing to thermal kinetic energy. Through the agency of momentum transfer or by strong interactions, the minimum energy packing of the long sulfonate-ended side chains is disrupted. This, in turn, creates more free volume that in turn causes $CO_2$ permeability to increase. As clusters are covalently coupled to the perfluorocarbon matrix, the main chains are disrupted thereby increasing long range segmental mobility which would promote an increase in permeability.

## CONCLUSIONS

Sol-gel reactions for $Zr(OBu)_4$ were conducted within the polar-nonpolar nanophase-separated morphology of water + ethanol-swollen Nafion sulfonic acid membranes. In these experiments, $Zr(OBu)_4$ monomer entered membranes having low water concentration from only one surface for different permeation times, followed by film drying. IR spectroscopic peaks reflecting $ZrO_2$ structure and incomplete hydrolysis of ZrOBu groups near both surfaces were detected. Vibrations characteristic of $Zr(OEt)_4$, due to alkoxy exchange in the presence of the solvent EtOH, were also detected near both sides. IR bands characteristic of both unreacted alkoxides are more distinct near the nonpermeated

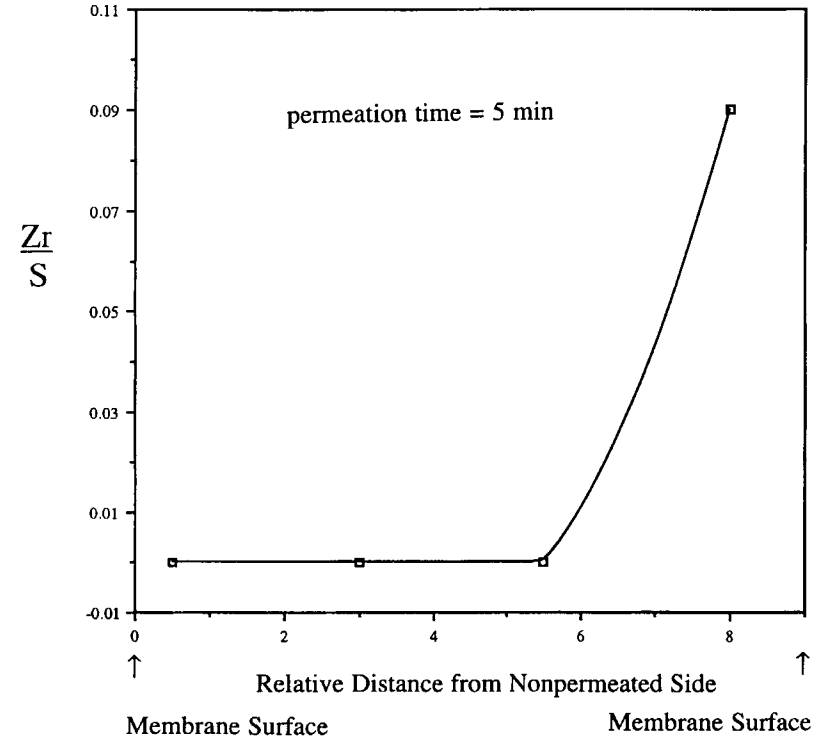


**Figure 4** Zr/S EDAX intensity ratio profile for a Nafion/[zirconium oxide] film for 5 min TBZ permeation time. The ends of the horizontal axis correspond to the film surfaces.

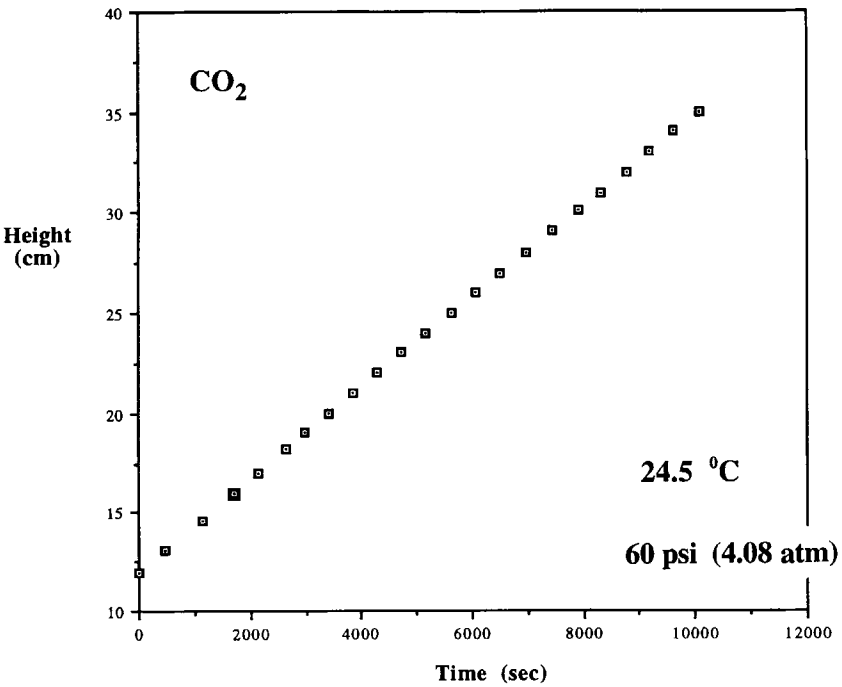


**Figure 5** Dye slug height in capillary tube versus time of $CO_2$ permeation for $p$ = 60 psig (4.08 atm) and 24.5°C.

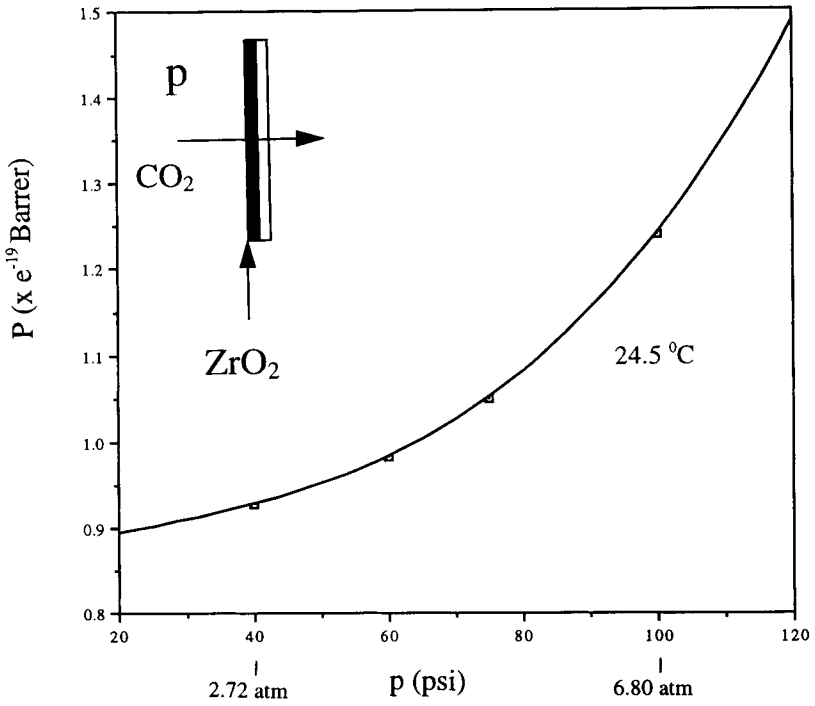


**Figure 6** $CO_2$ permeability coefficient versus pressure at 24.5°C for a Nafion/[zirconium oxide] film for which permeation time = 10 min.

brane thickness. An IR band for the ZnOBu group diminishes, whereas that for ZnOEt increases with increasing time near the permeated surface due to progressive alkoxy exchange. The $ZrO_2$ band becomes more intense with time near the TBZ-permeated surface. EDAX/SEM studies of Zr concentration across the membrane thickness verified zirconate compositional asymmetry. Thus, the primary goal of these investigations, namely to ascertain whether an asymmetric zirconium oxide phase can be affected, has been achieved. $CO_2$ gas permeability versus upstream pressure plots are monotonically increasing, suggesting diffusion accompanied by complex plasticization.

This work has been supported by a grant from the National Science Foundation/Electric Power Research Institute (Advanced Polymeric Materials, DMR-9211963). This work was also sponsored in part by the Air Force Office of Scientific Research, Air Force Systems Command, USAF, under grant number AFOSR F49620-93-1-0189. The U.S. Government is authorized to reproduce and distribute reprints for Governmental purposes notwithstanding any copyright notation thereon. The donation of Nafion membranes by the E. I. duPont de Nemours & Co., through the efforts of J. T. Keating, is appreciated.

## REFERENCES

1. D. C. Bradley, R. C. Mehrotra, and D. P. Gaur, *Metal Alkoxides*, Academic Press, New York, 1978 p.30.
2. D. C. Bradley and W. Wardlaw, *J. Chem. Soc.*, **73,** 280 (1951).
3. D. C. Bradley, in *Metal-Organic Compounds,* Symposium Series 23, American Chemical Society, Washington, D.C., 1959, pp. 10–36.
4. K. S. Mazdiyasni, C. T. Lynch, and J. S. Smith, *J. Amer. Ceram. Soc.*, **48**(7), 372 (1965).
5. K. S. Mazdiyasni, C. T. Lynch, and J. S. Smith, *J. Amer. Ceram. Soc.*, **50**(10), 532 (1967).
6. C. J. Brinker and G. W. Scherer, *Sol-Gel Science: The Physics and Chemistry of Sol-Gel Processing,* Academic Press: Boston, 1990 Ch. 2.
7. D. C. Bradley and D. G. Carter, *Canadian J. Chem.*, **39,** 1434 (1961).
8. D. C. Bradley and D. G. Carter, *Canadian J. Chem.*, **40,** 15 (1962).
9. B. E. Yoldas, *J. Am. Ceram. Soc.*, **65,** 387 (1982).
10. B. E. Yoldas, *J. Mat. Sci.*, **21,** 1080 (1986).
11. A. C. Pierre and D. R. Uhlmann, *Mat. Res. Soc. Symp. Proc.*, **121,** 207 (1988).
12. K. S. Mazdiyasni, C. T. Lynch, and J. S. Smith, *J. Amer. Ceram. Soc.*, **49,** 186 (1966).
13. M. T. Harris, C. H. Byers, and R. R. Brunson, *Mat. Res. Soc. Symp. Proc.*, **121,** 287 (1988).

14. D. Kundu and D. Ganguli, *J. Mat. Sci. Lett.*, **5,** 293 (1986).
15. T. D. Gierke, G. E. Munn, and F. C. Wilson, *J. Polym. Sci.: Polym. Phys. Ed.*, **19,** 1687 (1981).
16. R. V. Gummaraju, MS Thesis, University of Southern Mississippi, 1994.
17. K. A. Mauritz, R. F. Storey, and C. K. Jones, in *Multiphase Polymer Materials: Blends, Ionomers and Interpenetrating Networks,* ACS Symposium Series 395, L. A. Utracki and R. A. Weiss, Eds., American Chemical Society, Washington, D.C., 1989.
18. K. A. Mauritz and R. M. Warren, *Macromolecules,* **22,** 1730 (1989).
19. K. A. Mauritz, I. D. Stefanithis, S. V. Davis, R. W. Scheetz, R. K. Pope, G. L. Wilkes, and H-H. Huang, *J. Appl. Polym. Sci.,* **55,** 181 (1995).
20. P. L. Shao, K. A. Mauritz, and R. B. Moore, *Chem. Mater.,* **7,** 192 (1995).
21. P. L. Shao, R. B. Moore, and K. A. Mauritz, *J. Polym. Sci.: B. Polym. Phys. Ed.,* **34,** 873 (1996).
22. Q. Deng, R. B. Moore, and K. A. Mauritz, *Chem. Mater.,* **7,** 2259 (1995).
23. Q. Deng, R. B. Moore, W. M. Jarrett, and K. A. Mauritz, *J. Sol-Gel Sci. Technol.,* to appear.
24. Q. Deng, K. A. Mauritz, and R. B. Moore, in *Hybrid Organic-Inorganic Composites,* ACS Symposium Series 585, J. E. Mark, C. Y-C. Lee, and P. A. Bianconi, Eds., American Chemical Society, Washington, D.C., 1995.
25. S. V. Davis, K. A. Mauritz, and R. B. Moore, *Am. Chem. Soc. Polymer Prepr.,* **35**(1), 419 (1994).
26. M. Falk, in *Perfluorinated Ionomer Membranes,* ACS Symposium Series 180, A. Eisenberg and H. L. Yeager, Eds., American Chemical Society, Washington, D.C., 1982, p. 139.
27. M. Nogami, *J. Non-Cryst. Solids,* **69,** 415 (1985).
28. S. W. Lee and R. A. Condrate, *J. Mater. Sci.,* **23,** 2951 (1988).
29. N. T. McDevitt and W. L. Baun, *Spectrochem. Acta,* **20,** 799 (1964).
30. S. M. Sim, P-Y. Chu, R. H. Krabill, and D. E. Clark, in *Ultrastructure Processing of Advanced Ceramics,* J. D. Mackenzie and D. R. Ulrich, Eds., John Wiley and Sons, New York, 1988, p. 995.
31. Examples are found throughout J. Crank and G. S. Park, *Diffusion in Polymers,* Academic Press, London, 1968.

*Received January 9, 1996*
*Accepted April 5, 1996*